Improving the surface quality and mechanical properties of additively manufactured AISI 316L stainless steel by different surface post-treatment

Available online at www.sciencedirect.com

ScienceDirect

Procedia CIRP 118 (2023) 771–776

www.elsevier.com/locate/procedia

16th CIRP Conference on Intelligent Computation in Manufacturing Engineering, CIRP ICME '22, Italy

Improving the surface quality and mechanical properties of additively manufactured AISI 316L stainless steel by different surface post-treatment

Amir Behjat[a,b], Erika Lannunziata[b], Elżbieta Gadalińska[c], Luca Iuliano[b], Abdollah Saboori[b,*]

[a]*Department of Materials Engineering, Isfahan University of Technology, 84156-83111 Isfahan, Iran*

[b]*Integerated Additive Manufacturing Center (IAM@Polito), Department of Management and Production engineering, Politecnico di Torino, Corso duca degli Abruzzi 24, 10129, Torino, Italy*

[c] *Łukasiewicz Research Network – Institute of Aviation, Materials and Structures Research Center, Al. Krakowska 110/114, 02-256, Warszawa, Poland*

* Corresponding author. Tel.: +39-011-090-7285; E-mail address: Abdollah.saboori@polito.it

Abstract

Additive Manufacturing (AM) provides new insights into producing metallic components. Despite all the advantages of AM, two main challenges to its use are the high surface roughness and tensile residual stress of the AM samples in the as-built (AB) state. Therefore, this research aims to study the effect of different post surface treatments such as grinding, drag finishing and surface mechanical treatment on the surface quality of the 316L stainless steel parts produced by the laser powder bed fusion technique. The surface integrity and mechanical properties of AB and surface treated samples were analyzed and compared. Compared to the AB state, the surface roughness of the post-treated samples decreased, and their microhardness improved. In the case of residual stress, it is found that SMT could transform the initial tensile residual stress into compressive ones.

Keywords: Additive manufacturing; Surface mechanical treatment; 316L stainless steel; Selective laser melting; Residual stress

1. Introduction

Due to good mechanical properties and excellent corrosion resistance, AISI 316L has been widely used as a structural material in different applications such as aircraft components, medical implants, and petrochemical industries [1,2]. Metal additive manufacturing (AM) is an interesting/emerging method to fabricate complex shape components made of different alloys [3,4]. This technology allows engineers to design and produce components with complex geometries that can not be produced with traditional methods such as machining and casting [5,6]. Laser Powder Bed Fusion (L-PBF) process, also known as Selective Laser Melting (SLM), is one of the advanced powder-based AM processes that have received lots of attention [7,8]. In this process, metallic components are fabricated directly from starting powder in a layer by layer manner, generally by applying one or more high power laser beams [9,10]. In the L-PBF process, product quality strongly depends on the process parameters such as laser power, layer thickness, laser scanning speed, scan strategy and build orientation [11,12]. Over the last decades, several efforts have been undertaken to understand the role of each process parameter on the internal defects, surface roughness integrity, and mechanical properties of the metallic parts produced via the L-PBF process [13,14]. However, high surface roughness, residual porosity, large tensile residual stresses near the external surface, and columnar grains with anisotropic properties are still challenges that this technology faces [15,16]. In fact, these problems can increase the probability of crack formation/propagation in the components and, consequently, deteriorate the corrosion resistance [14,15], mechanical performance, and wear resistance of the as-built parts [17]. Therefore, several efforts have been undertaken to overcome these challenges and improve the performance of the AM parts. One of these efforts is the development of various post surface treatments that can solve lots of

10.1016/j.procir.2023.06.132

aforementioned issues. However, selecting an appropriate post-treatment technique should be performed properly considering the shape and dimensions of the part to be treated as well as the time and cost consumption to get appropriate properties [18–20].

Currently, an improvement of the surface properties of L-PBF fabricated 316L parts after the (finishing or polishing) surface mechanical post-treatment was confirmed [21,22] [ref]. In the surface mechanical treatment, modification of surface layers induced by severe plastic deformation provides the required surface roughness and improves mechanical properties such as microhardness, fatigue strength, and wear resistance. At present, very few studies have studied the effect of mechanical surface treatments on the surface quality of the metallic components produced via the L-PBF process [15,23]. For instance, Kumar et al. found that using the surface mechanical attrition treatment (SMAT) process makes it possible to achieve an improved surface roughness and hardness of the surface of the AISI 316L samples produced via the L-PBF process [24]. Portella et al. employed mechanical post-processing to improve residual stress distribution in L-PBF 316L stainless steel and found that the mechanical treatment can reduce the R_a value from 12 µm to 1.5 µm [21].

Previous studies have reported that the SMT process could affect the near-surface microstructure of the treated part. Indeed, the repeated impacts during the shot peening (SP) based treatment not only the microstructure is refined and the surface crystal defects increased but also induce compressive residual stress at the surface and subsurface regions, which affect the corrosion resistance and mechanical properties of treated substrate [18,21,24].

Currently, very few papers have focused on the effect of different post-treatments on the surface integrities and mechanical properties of L-PBF parts. Therefore, the current study presents a comprehensive experimental work implemented to study the influence of the different surface post treatments on the surface quality of the L-PBF manufactured 316L stainless steel in terms of microstructure and roughness, microhardness and residual stresses measurements.

2. Material and methods

2.1. Material and specimen preparation

AISI 316L stainless steel gas atomized powder, supplied by Oerlikon, was used as the feedstock material in this work. Fig 1 shows the particle size distribution of the starting powder particles. As it can be seen, the size of the powder particles lied in the range of 15-45 µm (d_{10}= 12.5 µm, d_{50}=21.2 µm, d_{90}=32.5 µm).

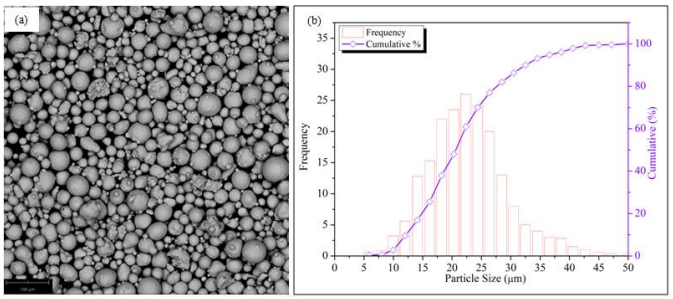

Fig. 1. a) SEM image of the initial powder; b) particle size distribution histograms of AISI 316L powders.

The AISI 316L samples were fabricated into cylindrical disks with a diameter of 12 mm and thickness of 3 mm using a Concept Laser Mlab Cusing-R machine equipped with a 100W fiber laser. The chamber was filled with high purity argon gas to minimize the risk of oxidation during the build process. A bidirectional stripe scanning pattern with a 67° angle rotation between each successive layer was used as the scanning strategy. The L-PBF process parameters of the 316L used in this work are given in table 1. The density evaluation of the samples in the as-built (AB) state revealed that all the specimens had a relative density of more than 99.5%.

Table 1: L-PBF processing parameters used in this work

Laser power [W]	95
Laser scan speed [mm/s]	500
Laser spot size [µm]	50
Layer thickness [µm]	25
Hatch distance [µm]	100

2.2. Surface post-treatment

In this work, three different post-processing methods, including surface grinding (G), drag finishing (DF), and surface mechanical treatment (SMT), are used to enhance the surface quality of L-PBF manufactured specimens. For the grinding treatment, the as-built surface of the samples was ground with SiC paper down to a 1200 grit finish. Instead, for the drag finishing operation, the as-built samples were treated for three hours at 200 rpm rotation speed using a ceramic abrasive media with a cylindrical shape. The SMT process which was implemented in this study was recirculating shot peening which was developed by Soyama et al. [25]. In this process, high-pressure water was injected from a special nozzle design to recirculate shots made of stainless steel or ceramics in the chamber, which produced severe plastic deformation via multidirectional and random shot impacts on the surface layer of the treated specimen. In this study, 250 zirconium oxide shots with average diameters of 5mm and hardness of 1100 Vickers were used. The pressure of the water jet was equal to 10 MPa, the standoff distance between the nozzle and the surface specimen was 30 mm, and the process duration was 20 min.

2.3. Material characterization

The surface morphology of the samples was characterized using a scanning electron microscope (SEM, JEOL, Japan) under the voltage of 15 kV. The top surface microhardness was measured using a Vickers indenter loaded by 0.025 kg.f, for a dwell time of 15 s. A total of five measurements were carried out at different treated zones, and the average values were reported together with their standard deviations.

Surface roughness was analyzed using a MarSurf RTP80 tester according to ISO 428/JIS 80601 standards for three times for each sample.

The XRD patterns were obtained on Philips X'pert MPD X-ray, which was operated at 40 kV/30 mA with Cu Kα radiation. The 2θ range of 40-80° with a step by step scanning length of 0.02° was set to obtain the X-ray diffraction data. The full width at half maximum (FWHM) of the diffraction θ peaks was also determined, and the crystallite sizes and microstrain were achieved utilizing the Williamson–Hall (W–H) method.

X-ray diffraction stress measurement was realized using the same radiation type and by applying the standardized $\sin^2\psi$ method based on the relative position of the diffraction peak hkl=(042), nominally appearing at the angular position 2θ=144.62°.

3. Results and discussions

3.1. Surface roughness

Fig. 2 shows the surface roughness and profile of the AISI 316L samples after different surface treatments. In fact, Fig. 2(a) compares the surface roughness profiles of the treated AISI 316L specimens with the AB one. The measured roughness parameters, *Ra*, *Rt* and *Rz*, of the AB and treated specimens are plotted and shown in Fig. 2 (b.c).

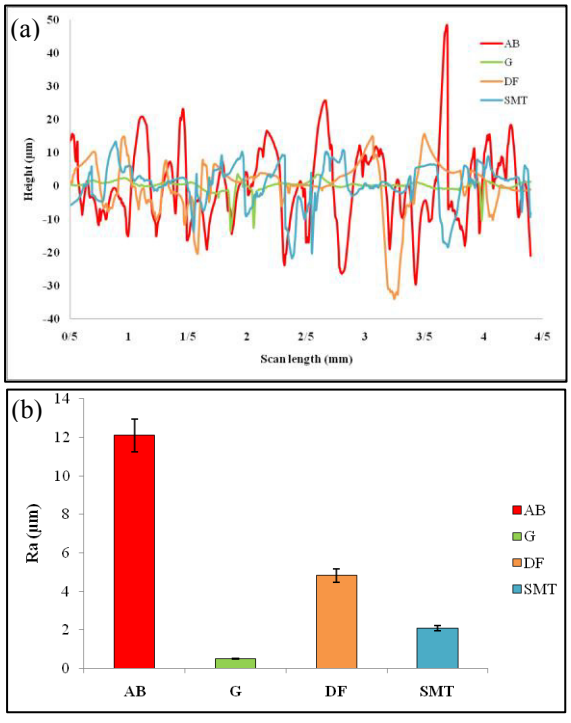

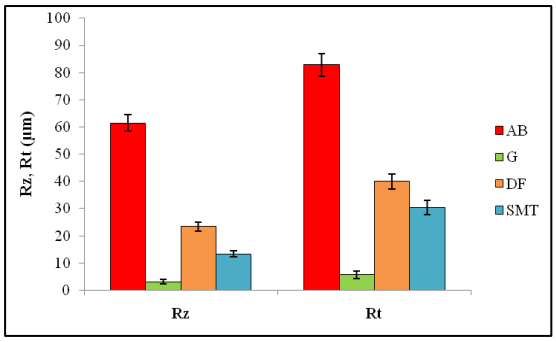

Fig. 2. (a) Surface roughness profiles; (b,c) Surface roughness parameters of the AB AISI 316L and after (G), (DF) and (SMT) processes.

It is observed that irregular and distorted profiles are formed for the AB sample due to the non-melted adhered powders on the surface. This trend of surface roughness is in line with what is reported for AISI 316L samples produced via the L-PBF process [18,21]. As shown in Fig. 2, there is an excessive difference between the surface roughness of the AB and post-processed specimens. The measured roughness of all of the post-treated samples exhibited a decreasing tendency. The lowest surface roughness values were obtained after the G operations and were approximately ten times lower than for the AB specimen. After DF, most surface defects, particularly partially melted powder stuck on the surface, were removed. For the SMT sample, most of the roughness peaks were removed or flattened so that the surface became much smoother, with some residual valleys. The slight waviness of the SMT surface is the result of the spherical dimples due to the impact of the steel balls. Indeed, the SMT not only reduces the height of the peaks on the surface but also fills valleys producing a smooth surface eventually [21,24].

3.2. Surface characteristics

Fig. 3 reveals the surface morphology of AB, G, DF and SMT L-PBF AISI 316L. It is obvious that there is a marked difference between the surfaces of these specimens. As shown in Fig. 3(a), the surface of AB is very rough and partially melted particles on the top surface are presented, which naturally affect the continuity of the surface. However, after different post-treatments, there is a significant difference between the treated surfaces with the AB specimen, and the partially melted particles disappeared from the surface. The results indicate that the G specimen represented a flat surface, and only grinding tracks are represented (Fig. 3(b)). As depicted in Fig. 3(c), DF operation resulted in partial removal and flattening of the highest asperities of the AB sample. The material removal from DF, with proper optimization parameters and appropriate ceramic media, could lead to smoother and less tortuous surface roughness and lower roughness [26]. In addition, the surface of the SMT samples, which is shown in Fig. 3(d), represents the regions of convexity and concave or dimple shape due to the impact of shots on the surface.

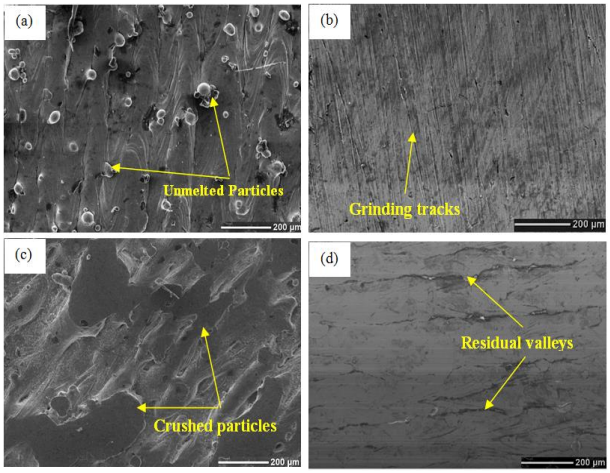

Fig. 3. SEM micrograph showing the top surface morphology of all samples, (a) AB; (b) G; (c) DF; (d) SMT.

The XRD patterns of the L-PBF AISI 316L before and after surface treatments are compared in Fig. 4 (a).

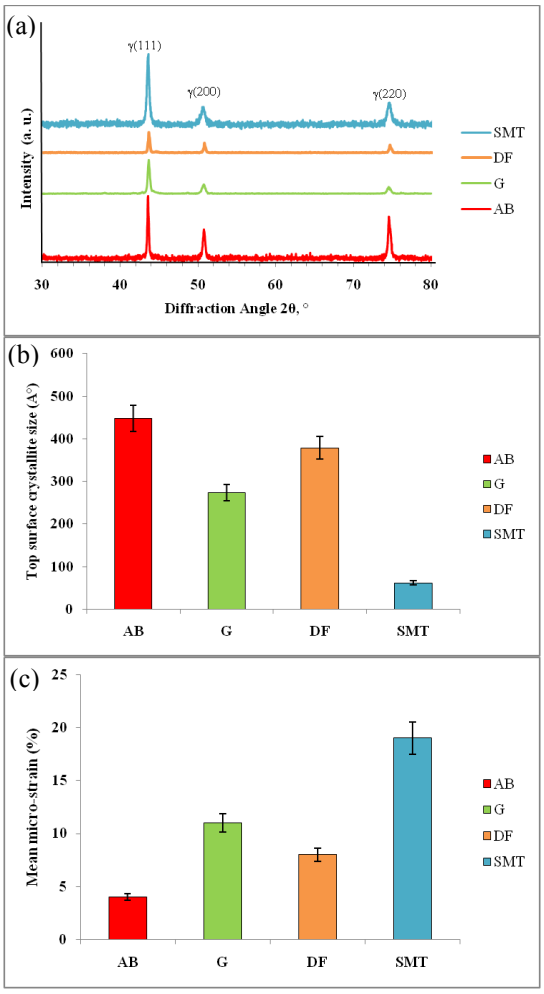

Fig. 4. a) XRD pattern of all the samples b) Top surface grain size; c) Measured micro-strain in all sets of specimens

As can be seen in Fig. 4(a), the dominant phase in all the samples is austenite. After SMT and DF treatments, there are no additional phases, and the locations of all peaks are the same as the sample before the treatments. It is evident that no α'-martensite (bcc, a=2.87 Å) was formed upon mechanical surface treatment. Meanwhile, it is shown that the diffraction peaks of the SMT samples become wider, which resulted from the refined domain sizes and increased microstrain on the surface induced by plastic deformation.

Based on the XRD analyses, variations of surface grain size and microstrain for the AB and treated specimens are summarized in Fig. 4 (b,c). As expected, SMT represented the lowest grain size and higher microstrain level on the top surface due to the plastic deformation. DF specimen exhibited the lowest microstrain level showing a slight difference from the AB sample. As mentioned in previous reports, the high crystal defects produced due to plastic deformation can retard or prohibit the initiation and propagation of microcracks, which may enhance the fatigue properties [27,28]. Therefore, it should be noted that SMT decreases the surface roughness and increases the microstrain and crystal defects, which is the development of a fully hardened structure on the top surface of the AM parts. This is consistent with the hardness, and residual stress findings explained further.

3.3. Hardness

The surface hardness of the AB and post surface treated samples are reported in Fig. 5.

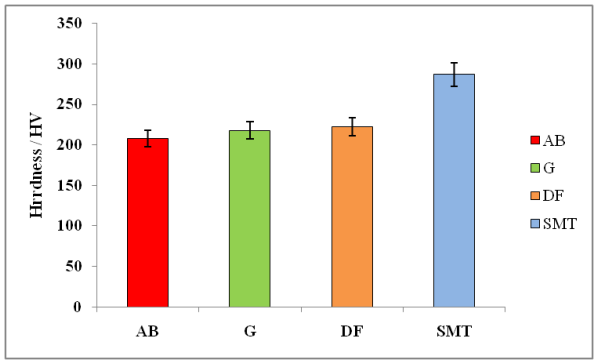

Fig. 5. Average top surface microhardness of the different samples.

A comparison between the microhardness of the AB sample with the microhardness of the samples after the surface treatment shows that the hardness of the SMT specimen is much higher than the AB and other post-processed AISI 316 L samples. The surface hardness of the G, DF and SMT samples are 218±23, 222±19, and 287±25 HV, respectively. The G treatment had the lowest effect on hardness increase due to the low kinetic energy of the mechanical treatment process. Based on XRD results and previous studies, the hardness increases can be attributed to the strain hardening and refinement of grains in severely deformed surface layers [21,24].

3.4. Superficial residual stress

Fig. 6 depicts the surface residual stresses obtained by XRD analysis for the AB and post-processed samples. The as-built sample shows tensile residual stresses up to 20-30 MPa. Simson et al. reported that residual stresses on the top surface

of the L-PBF 316L samples are approximatively equal to 200 MPa with an evolution from 100 to 150 MPa in the sample's thickness. They reported that the magnitude of the surface residual stress highly depend on L-PBF parameters [29]. As reported by several researchers, Mostly tensile residual stresses can be observed in the AB sample which have detrimental effects on mechanical properties by facilitating crack initiation and propagation [21,24,25] and corrosion resistance [30,31]. As shown in Fig 6, the surface residual stresses of -95 and -18 MPa were measured in G and DF samples, respectively. Compressive residual stress of -230 MPa was generated on the top surface of the SMT sample. For the post surface treated samples, the residual stress of the DF specimens are higher than the G and SMT specimens. There is compressive residual stress for G and SMT compared to the as-built L-PBF manufactured specimen.

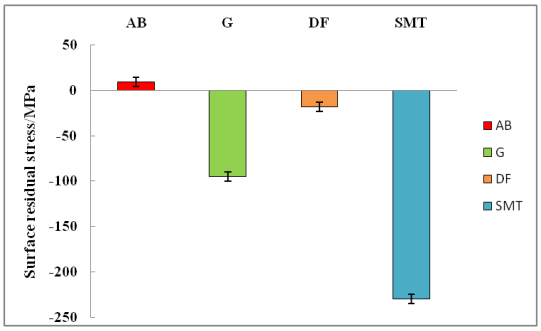

Fig. 5. Average top surface residual stress of the different samples.

Actually, SMT was found to be the most efficient treatment for inducing compressive residual stresses on the surface. In agreement with the surface residual stress results and in the confirmation of previous research findings, this behaviour implies that the randomly impact of several shot balls repeatedly and concurrently on the surface of a workpiece during the process of SMT leads to the higher compressive residual stress in the near surface layers [21]. The microhardness results presented in the previous section support this finding.

4. Conclusion

In this study, the effect of post-process operations on the surface characteristic of AISI 316L specimens manufactured by the L-PBF method is investigated. The main conclusions that can be drawn based on the key findings in this work are as follow:

- The surface roughness analysis of the samples reveals a remarkable decrease in the surface roughness after the post treatments.
- The XRD analysis confirmed the development of the austenite phase in all the samples. Even the SMT process did not lead to the formation of martensite phase, caused grain refinement and increased local microstrain.
- Microhardness at the top surface can be enhanced significantly due to the strain hardening and grain refinement produced by SMT.
- Residual stresses measurements show that G and DF were not as efficient as the SMT process in changing the initial tensile residual stress.

All in all, it can be concluded that SMT as a post surface treatment can be an effective method to improve the surface inherited from the L-PBF process.

References

[1] A. Saboori, A. Aversa, F. Bosio, E. Bassini, E. Librera, M. De Chirico, S. Biamino, D. Ugues, P. Fino, M. Lombardi, An investigation on the effect of powder recycling on the microstructure and mechanical properties of AISI 316L produced by Directed Energy Deposition, Mater. Sci. Eng. A. (2019) 138360. https://doi.org/https://doi.org/10.1016/j.msea.2019.138360.

[2] L. Chen, B. Richter, X. Zhang, K.B. Bertsch, D.J. Thoma, F.E. Pfefferkorn, Effect of laser polishing on the microstructure and mechanical properties of stainless steel 316L fabricated by laser powder bed fusion, Mater. Sci. Eng. A. 802 (2021). https://doi.org/10.1016/j.msea.2020.140579.

[3] M. Aristizabal, P. Jamshidi, A. Saboori, S.C. Cox, M.M. Attallah, Laser powder bed fusion of a Zr-alloy: Tensile properties and biocompatibility, Mater. Lett. 259 (2020) 126897. https://doi.org/10.1016/J.MATLET.2019.126897.

[4] M.H. Mosallanejad, B. Niroumand, A. Aversa, D. Manfredi, A. Saboori, Laser Powder Bed Fusion in-situ alloying of Ti-5%Cu alloy: Process-structure relationships, J. Alloys Compd. (2020) 157558. https://doi.org/https://doi.org/10.1016/j.jallcom.2020.157558.

[5] L.E. Murr, S.M. Gaytan, D.A. Ramirez, E. Martinez, J. Hernandez, K.N. Amato, P.W. Shindo, F.R. Medina, R.B. Wicker, Metal Fabrication by Additive Manufacturing Using Laser and Electron Beam Melting Technologies, J. Mater. Sci. Technol. 28 (2012) 1–14. https://doi.org/10.1016/S1005-0302(12)60016-4.

[6] T. Souflas, H. Bikas, M. Ghassempouri, A. Salmi, E. Atzeni, A. Saboori, I. Brugnetti, A. Valente, F. Mazzucato, P. Stavropoulos, A comparative study of dry and cryogenic milling for Directed Energy Deposited IN718 components: effect on process and part quality, Int. J. Adv. Manuf. Technol. 119 (2022) 745–758. https://doi.org/10.1007/s00170-021-08313-7.

[7] M.R. Jandaghi, A. Saboori, L. Iuliano, M. Pavese, On the effect of rapid annealing on the microstructure and mechanical behavior of additively manufactured stainless steel by Laser Powder Bed Fusion, Mater. Sci. Eng. A. 828 (2021) 142109. https://doi.org/https://doi.org/10.1016/j.msea.2021.142109.

[8] A. Saboori, A. Aversa, G. Marchese, S. Biamino, M. Lombardi, P. Fino, Microstructure and Mechanical Properties of AISI 316L Produced by Directed Energy Deposition-Based Additive Manufacturing: A Review, Appl. Sci. 10 (2020). https://doi.org/10.3390/app10093310.

[9] M. Dadkhah, M.H. Mosallanejad, L. Iuliano, A. Saboori, A Comprehensive Overview on the Latest Progress in the Additive Manufacturing of Metal Matrix Composites: Potential, Challenges, and Feasible Solutions, Acta Metall. Sin. (English Lett. 34 (2021) 1173–1200. https://doi.org/10.1007/s40195-021-01249-7.

[10] R. Barros, F.J.G. Silva, R.M. Gouveia, A. Saboori, G. Marchese, S. Biamino, A. Salmi, E. Atzeni, Laser powder bed fusion of inconel 718: Residual stress analysis before and after heat treatment, Metals (Basel). 9 (2019). https://doi.org/10.3390/met9121290.

[11] R. Chai, Y. Zhang, B. Zhong, C. Zhang, Effect of scan speed on grain and microstructural morphology for laser additive manufacturing of 304 stainless steel, Rev. Adv. Mater. Sci. 60

(2021) 744–760. https://doi.org/10.1515/rams-2021-0068.

[12] M.H. Mosallanejad, B. Niroumand, A. Aversa, A. Saboori, In-situ alloying in laser-based additive manufacturing processes: A critical review, J. Alloys Compd. 872 (2021) 159567. https://doi.org/https://doi.org/10.1016/j.jallcom.2021.159567.

[13] H. Sohrabpoor, V. Salarvand, R. Lupoi, Q. Chu, W. Li, B. Aldwell, W. Stanley, S. O'Halloran, R. Raghavendra, C.H. Choi, D. Brabazon, Microstructural and mechanical evaluation of post-processed SS 316L manufactured by laser-based powder bed fusion, J. Mater. Res. Technol. 12 (2021) 210–220. https://doi.org/10.1016/J.JMRT.2021.02.090.

[14] M.A. Melia, J.G. Duran, J.R. Koepke, D.J. Saiz, B.H. Jared, E.J. Schindelholz, How build angle and post-processing impact roughness and corrosion of additively manufactured 316L stainless steel, Npj Mater. Degrad. 4 (2020). https://doi.org/10.1038/s41529-020-00126-5.

[15] E. Maleki, S. Bagherifard, M. Bandini, M. Guagliano, Surface post-treatments for metal additive manufacturing: Progress, challenges, and opportunities, Addit. Manuf. 37 (2021) 101619. https://doi.org/10.1016/J.ADDMA.2020.101619.

[16] M. Roccetti Campagnoli, M. Galati, A. Saboori, On the processability of copper components via powder-based additive manufacturing processes: Potentials, challenges and feasible solutions, J. Manuf. Process. 72 (2021) 320–337. https://doi.org/https://doi.org/10.1016/j.jmapro.2021.10.038.

[17] M. Benedetti, E. Torresani, M. Leoni, V. Fontanari, M. Bandini, C. Pederzolli, C. Potrich, The effect of post-sintering treatments on the fatigue and biological behavior of Ti-6Al-4V ELI parts made by selective laser melting, J. Mech. Behav. Biomed. Mater. 71 (2017) 295–306. https://doi.org/10.1016/j.jmbbm.2017.03.024.

[18] Y. Sun, R. Bailey, A. Moroz, Surface finish and properties enhancement of selective laser melted 316L stainless steel by surface mechanical attrition treatment, Surf. Coatings Technol. 378 (2019). https://doi.org/10.1016/j.surfcoat.2019.124993.

[19] H.M. Khan, Y. Karabulut, O. Kitay, Y. Kaynak, I.S. Jawahir, Influence of the post-processing operations on surface integrity of metal components produced by laser powder bed fusion additive manufacturing: a review, Mach. Sci. Technol. 25 (2020) 118–176. https://doi.org/10.1080/10910344.2020.1855649.

[20] C. Ye, C. Zhang, J. Zhao, Y. Dong, Effects of Post-processing on the Surface Finish, Porosity, Residual Stresses, and Fatigue Performance of Additive Manufactured Metals: A Review, J. Mater. Eng. Perform. 30 (2021) 6407–6425. https://doi.org/10.1007/s11665-021-06021-7.

[21] Q. Portella, M. Chemkhi, D. Retraint, Influence of Surface Mechanical Attrition Treatment (SMAT) post-treatment on microstructural, mechanical and tensile behaviour of additive manufactured AISI 316L, Mater. Charact. 167 (2020). https://doi.org/10.1016/j.matchar.2020.110463.

[22] S.M. Basha, M. Bhuyan, M.M. Basha, N. Venkaiah, M.R. Sankar, Laser polishing of 3D printed metallic components: A review on surface integrity, in: Mater. Today Proc., Elsevier Ltd, 2019: pp. 2047–2054. https://doi.org/10.1016/j.matpr.2020.02.443.

[23] J. Zhang, Y.J. Lee, H. Wang, A Brief Review on the Enhancement of Surface Finish for Metal Additive Manufacturing, 2021.

[24] V. Kumar, M.D. Joshi, C. Pruncu, I. Singh, S.S. Hosmani, Microstructure and Tribological Response of Selective Laser Melted AISI 316L Stainless Steel: The Role of Severe Surface Deformation, J. Mater. Eng. Perform. 30 (2021) 5170–5183. https://doi.org/10.1007/s11665-021-05730-3.

[25] H. Soyama, F. Takeo, Effect of Various Peening Methods on the Fatigue Properties of Titanium Alloy Ti6Al4V Manufactured by Direct Metal Laser Sintering and Electron Beam Melting, Materials (Basel). 13 (2020) 2216. https://doi.org/10.3390/ma13102216.

[26] Y. Kaynak, O. Kitay, The effect of post-processing operations on surface characteristics of 316L stainless steel produced by selective laser melting, Addit. Manuf. 26 (2019) 84–93. https://doi.org/10.1016/j.addma.2018.12.021.

[27] L. Denti, E. Bassoli, A. Gatto, E. Santecchia, P. Mengucci, Fatigue life and microstructure of additive manufactured Ti6Al4V after different finishing processes, Mater. Sci. Eng. A. 755 (2019) 1–9. https://doi.org/10.1016/j.msea.2019.03.119.

[28] M.A. Mahmood, D. Chioibasu, A.U. Rehman, S. Mihai, A.C. Popescu, Post-Processing Techniques to Enhance the Quality of Metallic Parts Produced by Additive Manufacturing, Metals (Basel). 12 (2022). https://doi.org/10.3390/met12010077.

[29] T. Simson, A. Emmel, A. Dwars, J. Böhm, Residual stress measurements on AISI 316L samples manufactured by selective laser melting, Addit. Manuf. 17 (2017) 183–189. https://doi.org/10.1016/j.addma.2017.07.007.

[30] G. Sander, A.P. Babu, X. Gao, D. Jiang, N. Birbilis, On the effect of build orientation and residual stress on the corrosion of 316L stainless steel prepared by selective laser melting, Corros. Sci. 179 (2021). https://doi.org/10.1016/j.corsci.2020.109149.

[31] G. Sander, S. Thomas, V. Cruz, M. Jurg, N. Birbilis, X. Gao, M. Brameld, C.R. Hutchinson, On The Corrosion and Metastable Pitting Characteristics of 316L Stainless Steel Produced by Selective Laser Melting, J. Electrochem. Soc. 164 (2017) C250–C257. https://doi.org/10.1149/2.0551706jes.